A Low Computational Approach for Assistive Esophageal Adenocarcinoma and Colorectal Cancer Detection

Zheqi Yu[1], Shufan Yang[2], Keliang Zhou[2], and Amar Aggoun[1]

[1] Faculty of Science and Engineering, University of Wolverhampton, Wolverhampton, UK,
[2] School of Engineering, University of Glasgow, Glasgow, UK,

Abstract. In this paper, we aim to develop a low-computational system for real-time image processing and analysis in endoscopy images for the early detection of the human esophageal adenocarcinoma and colorectal cancer. Rich statistical features are used to train an improved machine-learning algorithm. Our algorithm can achieve a real-time classification of malign and benign cancer tumours with a significantly improved detection precision compared to the classical HOG method as a reference when it is implemented on real time embedded system NVIDIA TX2 platform. Our approach can help to avoid unnecessary biopsies for patients and reduce the over diagnosis of clinically insignificant cancers in the future.

Keywords: Machine learning, Endoscopy, Cancer detection, Texture analysis division.

1 Introduction

Although esophageal adenocarcinoma is uncommon, its diagnosis has increased dramatically over the past 25 years [1]. During diagnosis process, information obtained from the patients physical examination, laboratory data, and endoscopic evaluation help doctors to make the correct diagnosis. While those diagnosis process, medical image processing analysis has become more and more popular in an early stage due to low cost [2]. However, using endoscopic images to detect the lesion of esophageal adenocarcinoma and colorectal cancer is a challenging task due to several facts presented in the endoscopy pictures: air bubbles, ink marking, uneven illumination and shadows [3]. Conventional medical image processing algorithm design includes the following steps: image segmentation, feature extraction, reduction and classification.

Artificial neural network based image segmentation approaches have drawn a lot of attention due to their signal-to-noise independency. However, while those approaches can achieve a high level of accuracy, they are computationally expensive with less than 10 frames per second in the latest literature [4] [5]. In this paper, we focus on the implementation of texture analysis as feature extractions into a machine learning classifier whilst balancing the computational

requirement and detection accuracy. We verify our low computational method for esophageal adenocarcinoma cancer detection using NVIDIA TX2 board. Experimental results show that the proposed algorithm can effectively improve the speed and accuracy by 20% compared with the HOG reference design.

2   Our Texture analysis based algorithm

In this paper, we use the texture analysis to extract and analyse the image grey levels for the spatial distribution pattern. A statistical histogram of features is calculated based on the Histograms of Oriented Gradients (HOG) [6] algorithm, followed by an AdaBoost classifier. Fig.1 shows the diagram of system structure blocks.
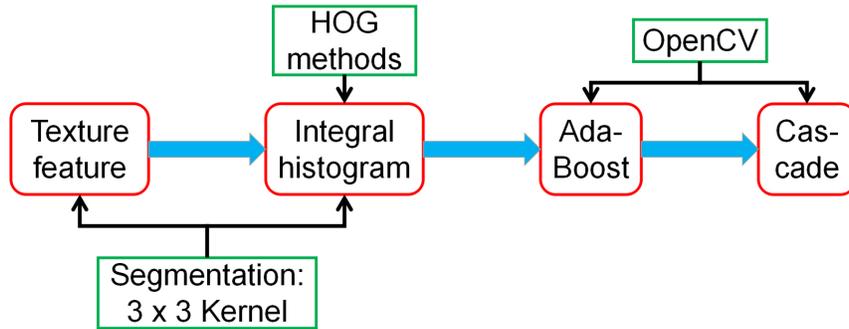

Fig. 1. Algorithm work flow diagram.

	Proposed Algorithm Procedure
1	**for** all pixel (i , j) in image I
2	magnitude = abs(I (i-1 , j-1) + I (i-1 , j) + I (i-1 , j+1) + I (i , j-1)
	−I (i , j)*8+ I (i , j+1) + I (i+1 , j-1) + I (i+1 , j) + I (i+1 , j+1))/8
3	bin = I (i , j) / (256/9); // uniform grey levels division or cubic-bezier curve grey levels
	division for different grey values range.
4	cell = getcell (i , j)
5	histogram (cell, bin) = histogram (cell , bin) + magnitude
6	**end**
7	**for** all cells c in image I
8	descriptor (c) = createblock (histogram)
9	descriptor (c) = integrated (descriptor (c))
10	**end**
11	**for** all detect i on windows w in image I
12	finaldesc = gatherHOG (descriptor , w)
13	results = AdaBoost (finaldesc , model)
14	**end**

Fig. 2. Pseudo code for proposed algorithm procedure.

Our algorithm first uses the 3x3 kernel to calculate each pixel in the kernel to get the texture feature, and then it calculates the corresponding grey division interval levels along with the kernel texture features. This process means the centre points will be greyscaled range division when the texture feature is calculating the surrounding pixels. For the statistical analysis, each pixel corresponds to a division grey interval in the statistical histogram. While the histogram is calculating, the algorithm adds all the texture features of the same grey level interval and then inputs result into the AdaBoost classifier through the HOG fast integral image method. Finally, all of the weak classifiers are cascaded to obtain a strong classifier.

Fig.2 is a pseudo code diagram for our proposed algorithm procedure; it has shown the grey levels division methods for how to work in the texture analysis.

3   Texture Analysis for Feature Calculation

Unlike natural images, medical images include rich texture information, such as widely used X-rays and cellular imaging. In image analysis, textures are interpreted as a repetitive arrangement of a basic pattern (hue primitives). Thus the description of a texture includes the colour tones that make up the texture and the relationship between the hues [7]. A texture is a regional feature and thus relates to the size and shape of an area, with the boundary between two texture patterns determined by examining the difference in greyscale pixel values [8]. Finally, a texture feature is a reflection of the object structure, and therefore can provide important image information about the object such as density, which is an essential method of image segmentation, feature extraction, classification and recognition.

In this paper, we propose a low computational approach of only using texture information in greyscale images based on an Neighbourhood Grey-tone Difference Matrix (NGTDM) algorithm.

The NGTDM method is used to depict the pixel values relationship with its surrounding [9]. The calculation equation is shown in equation (1).

$$\overline{A}(k,l) = \frac{1}{W^2 - 1} \left[\sum_{m=-d}^{d} \sum_{n=-d}^{d} f(k+m, l+n) \right]$$
$$where \qquad W = 2d+1, (m,n) \neq (0,0)$$

(1)

The W is general settings 3 or 5 that means take the W x W window size of the kernel; where d specifies the neighbourhood size of pixel distance. A 3x3 (W =3) kernel is used to calculate a pixel A in the graph whose column matrix of array coordinates is (k,l), and the pixel grey value also corresponds to the groups of different levels. For a two-dimension image, there should be 8 pixels around the pixel $\overline{A}$, to sum of the absolute value of the difference between a grey value (0-255) of the center pixel and the grey value of the surrounding pixels, in order to obtain the sequence $S(i)$ and put the result into the histogram calculation.

Where $f(k,l)$ is the grey value of the image in the window of central pixel $i(k,l)$. $S(k,l)$ represents the sum of the absolute values of the differences between the centre pixel i and the surrounding pixels.

$$S\left(k,l\right) = \sum \left|i - \overline{A}\left(k,l\right)\right| \qquad for \qquad f\left(k,l\right) = i \qquad (2)$$

In this paper, we calculate the histogram through the HOG method after the texture feature is extracted. But the gradient vector feature of HOG is replaced by the texture features to reduce computation complexity. Three different methods are proposed here: texture analysis based on HOG division (TAH), texture analysis based on uniform grey levels division (TAD) and texture analysis based on cubic-bezier curve grey levels division (TAC). As shown in Table 1, the TAH is a texture feature calculated directly by HOG histograms. The TAD is an improved method of replacing the gradient direction of HOG histograms. The TAC is calculated using cubic-bezier curve division to divide the grey bin levels of HOG histogram calculation.

Histogram statistics can be used to count any image features (such as greyscale, gradient and direction). The pixel's greyscale range contains 256 values [0 255], which are divided into sub-regions (called bins). Where n bins are divided, its' statistic pixel calculation result into a matched bin.

Our proposed TAD method classifies greyscale values into ranges without calculating the gradient directions. The greyscale range of 0-255 is divided into nine categories with the boundary ranges rounded down to the nearest whole number. Each divided range details as following:

$$range = bin_1 \cup bin_2 \cup .... \cup bin_n$$
$$(nbins = 9) \qquad (3)$$

$$[0, 255] = [0, 27] \cup [28, 56] \cup [57, 85] \cup [86, 113] \cup [114, 141]$$
$$\cup [142, 170] \cup [171, 198] \cup [199, 226] \cup [227, 255] \qquad (4)$$

The TAC is similar to the TAD method, but it has the non-uniform division greyscale range to 9 bins ($nbins = 9$) by the cubic-bezier curve equation B(t) (equation (5)).

$$B\left(t\right) = P_0\left(1-t\right)^3 + 3P_1 t\left(1-t\right)^2 + 3P_2 t^2\left(1-t\right) + P_3 t^3 \qquad t \in [0,1] \qquad (5)$$

P0 is the starting point of the curve (0, 0)
P3 is the end of the curve (255,255)
P1 and P2 are the control points for the trend of the curve, so any changing by these two parameters.
t is a dummy parameter that acts on all connected lines of points.

Table 1. Division Calculation Complexity Comparison table.

Types	Feature		Division Calculation Complexity
HOG	Histogram of Oriented Gradient of 3x3 cells (cell similar to kernel) gradient magnitude and gradient direction	The gradient of each pixel, including size and direction, all of the cell of gradients are divided into 9 bins that to get 9 dimensional feature vector.	Twice addition and subtraction + Once division calculation + Once arc-tangent function (mainly time consumption) + Once multiplication calculation
TAH			
TAD	Texture analysis for a 3x3 kernel	Central pixel of value to continuous uniform division for 9 bins	Once multiplication calculation + Once shiftoperation
TAC		Central pixel of value to cubic-bezier curve division for 9 bins	

The cubic-bezier also is called as a third-order Bezier; it is a classic method of curve approximation. In the endoscopic image analysis, the appearance of cancer, illumination condition changes and the background of the image have relatively small variability. The high and low light regions can be set up as different greyscale divided interval by curve regulation. Such as the highlighted area for low recognition rate, where the curve can be set smooth or steep to enhance the effect. And also, the same applies to low light area settings. There is an advantage than the uniform division that more suitable for the endoscopic environment.

The comparison of various features is shown in the following Table 1. Four methods are based on different classification and feature extraction. The HOG and TAH methods are both for using HOG division method for feature extraction. It uses greyscale pixel values for vector computation to separate the vector space results (vector directional angles) and to calculate gradient magnitude and gradient direction to histogram statistic. We can find on the TAD and TAC division methods that the kernel calculation is a texture analysis to the histogram statistics. It can achieve the greyscale values by calculating the difference values of pixels.

4   Experiments Results and Discussions

The experiment uses OpenCV 2.4.13 library version of AdaBoost traincascade program interface and runs on CPU i7 4710MQ for training and testing of the

above four methods. The final experiments are implemented on NVIDIA TX2 platform. We choose and set the 5 scale rates for the AdaBoost that are 1.05, 1.1, 1.3, 1.5 and 1.9. In order to eliminate differences from the OpenCV program optimisation for above four methods, we run the experiments using a unified single-threaded processing. We use VIVO Endoscopic Video Datasets [10] to train and test our proposed algorithm.
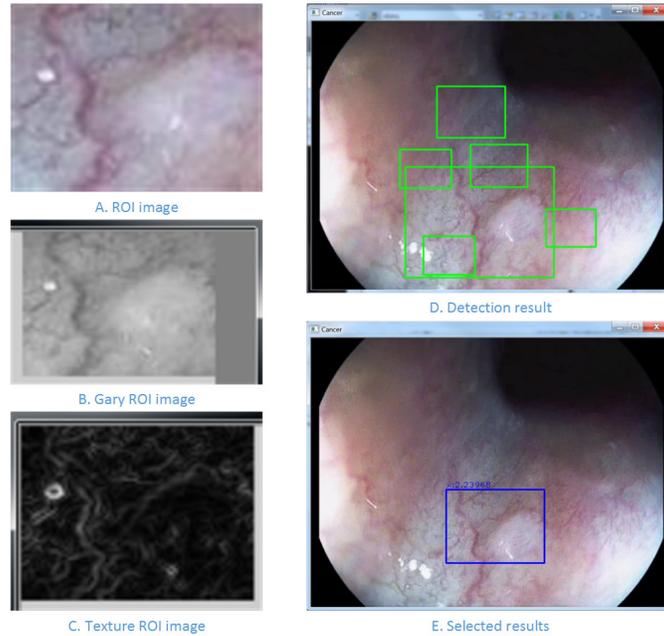
4.1   Quality results

Fig. 3. Computer simulation results.

After getting the statistical texture information, we need to decide the size of the bounding box (Region of Interests). A $K-means$ clustering algorithm is then used for clustering analysis esophageal adenocarcinoma cancer size on the endoscopy image that to sets a suitable detection window size, it is concluded to be 80 (width) x 60 (height), which is to obtain statistically the number of boxes (number of clusters) and the object size (cluster centre box). A simple AdaBoost classifier was online trained. However first experiments results show that the false detecting rate is too high due to the inefficient AdaBoost classifier, as shown in the Fig.3D.

In the second experiment, a cascade AdaBoost classifier uses the sliding window to find the objects in different positions of the image and magnify the

detection window to find the different size objects in the image with a threshold banding. The final object box is the highest score of the levelWeight by comparison. The final detection effect is shown on the Fig.3E.

4.2 Quantitative Analysis

Table 2 demonstrates the detection performance including precision and recall. For the precision results, there is many similarities, but the TAC algorithm more stable for each scale rate and it is the top average in the precision. For the recall results, the HOG division method (HOG and TAH) has a significant difference and lower than our design algorithm. The TAC is still top one in the average recall and each scale rate better than 10% with HOG division method. The result of comprehensive speed and recognition rate can meet the requirements of real-time operation for the algorithm after the 1.3 scale rate of AdaBoost. Moreover, in the embedded system test, the TAC method can be achieved in real time processing in the 1.9 scale rate (shown in the TACT results). The TAC method clearly dominates the best effect at this time scale rate.

Table 2. Precision and Recall Comparison table

Algorithm / Type Results	Scale rate	HOG	TAH	TAD	TAC	TACT
Precision (%)	1.05	65.4	49.7	60.5	64.3	61.5
	1.1	77.1	58.4	62.7	67.2	63.4
	1.3	75.1	67.6	68.7	71.8	64.1
	1.5	39.1	60.6	68.2	70.9	64.5
	1.9	66.4	61.2	66.8	66.6	59.5
Avg-Precision		64.42	59.50	65.38	68.16	62.60
Recall (%)	1.05	50.1	37.1	59.5	61.3	59.5
	1.1	55.9	48.7	62.8	63.5	62.0
	1.3	59.4	52.4	66.3	65.8	60.1
	1.5	39.7	45.4	60.6	63.7	56.6
	1.9	44.2	37.1	53.5	52.5	47.8
Avg -Recall		49.86	44.14	60.54	61.36	57.20

Fig.4 has compared the average processing speed. All of test videos and pictures are based on 640x480 resolution. In the 1.9 scale rate, the grey value division method is 10% faster than the HOG algorithm. Also, the TACT results have shown the embedded systems achieved real time processing that over the 25fps in the TX2 board.

Fig.5 has shown four algorithms of 9bins histogram statistics for the same image. By comparison, the TAC method of the histogram is outperformed by using the cubic-bezier curves for non-uniform greyscale range division. So that means each bin in the TAC is including a different greyscale range for the matched non-uniform grey interval and that can improve histogram differences. The TAH and

TAD methods of the histogram are smooth and stable which means there is litter different in features.
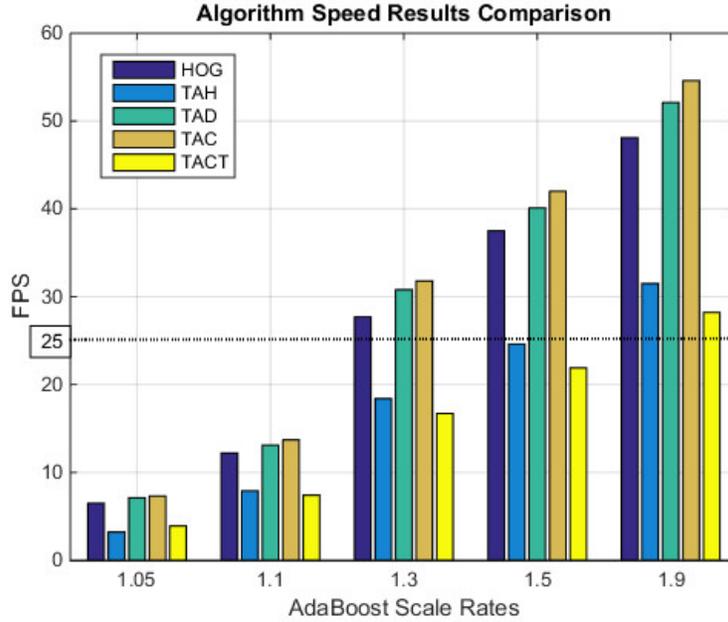

Fig. 4. Algorithm fps results.

4.3   Discussion

The TAC algorithm achieves the highest recognition rates, particularly when using higher scale rates compared to HOG algorithms. The HOG algorithms produce high levels of accuracy in esophageal cancer detection but have low recall rates (less than 50%). The TAH directly using texture features to match the official HOG calculation method, not only leads to a decrease in accuracy, but the processing speed also drops dramatically and as a result is unable to meet the requirements of the real-time processing. The use of the greyscale division method between the texture analysis and histogram, not only shows a higher accuracy (large-scale rate of AdaBoost setting) than the HOG method, but also a greater speed. In two Greyscale division methods, it has also been shown the best results from a non-uniform division using cubic-bezier curves. It means that in the textural analysis of cancer detection, the non-uniform range of greyscale values is good for histogram statistics. Therefore, it is possible that using the non-uniform intervals of greyscale values calculated by the cubic-bezier curve is better than the HOG algorithm for esophageal cancer detection. In
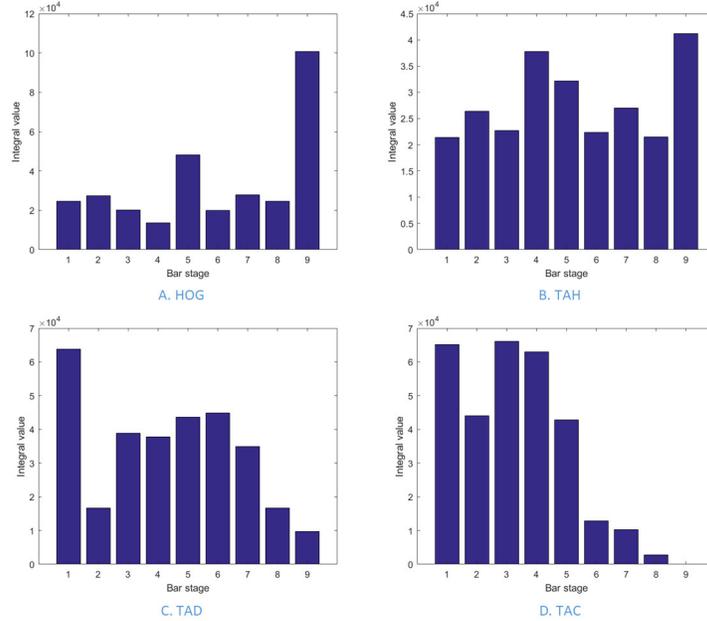
Fig. 5. Algorithm histogram results.

addition, in the embedded system, the processing without vector feature can reduce computation that helps it running fast and easy to achieve real time processing.

However, when using small-scale rates, the HOG method still provides the best accuracy using multi-feature calculation (vector of gradient and angle). This means that the texture analysis method for feature extraction mainly benefits from using a simplified calculation to reduce processing time, whilst sacrificing accuracy as a result. Our proposed TAC method has improved accuracy over traditional texture analysis methods, but is still limited by its use of simplified calculations in texture analysis.

5   Conclusion

In this paper, we proposed a supervised machine learning method integrated with texture analysis for medical image processing. We compared three different HOG based feature extraction techniques with our proposed non-uniform division method, and verified them in the embedded system platform. The computational cost of the HOG based technologies in supervised learning is high due to the processing needs for vector-based feature extraction. Our method takes advantage of dividable uneven greyscale levels presented in texture features to reduce the computational complexity of machine learning, enabling higher processing speed per second.

References

1. Lucy Sun, Amy F. Subar, Claire Bosire, Sanford M. Dawsey, Lisa L. Kahle, Thea P. Zimmerman, Christian C. Abnet, Ruth Heller, Barry I. Graubard, and Michael B. Cook. Dietary flavonoid intake reduces the risk of head and neck but not esophageal or gastric cancer in us men and women. *The Journal of nutrition*, 147(9):1729–1738, 2017.
2. Priya Darshini Velusamy and Porkumaran Karandharaj. Medical image processing schemes for cancer detection: A survey. In *Green Computing Communication and Electrical Engineering (ICGCCEE), 2014 International Conference on*, pages 1–6. IEEE, 2014.
3. TF Watson, MAA Neil, R. Jukaitis, RJ Cook, and T. Wilson. Videorate confocal endoscopy. *Journal of microscopy*, 207(1):37–42, 2002.
4. Jin Qi, Miao Le, Chunming Li, and Ping Zhou. Global and local information based deep network for skin lesion segmentation. *arXiv preprint arXiv:1703.05467*, 2017.
5. Zhen Yu, Xudong Jiang, Tianfu Wang, and Baiying Lei. Aggregating deep convolutional features for melanoma recognition in dermoscopy images. In *International Workshop on Machine Learning in Medical Imaging*, pages 238–246. Springer, 2017.
6. Navneet Dalal and Bill Triggs. Histograms of oriented gradients for human detection. In *2005 IEEE Computer Society Conference on Computer Vision and Pattern Recognition (CVPR'05)*, volume 1, pages 886–893. IEEE, 2005.
7. Nalini Bhushan, A. Ravishankar Rao, and Gerald L. Lohse. The texture lexicon: Understanding the categorization of visual texture terms and their relationship to texture images. *Cognitive Science*, 21(2):219–246, 1997.
8. Peter W. Hawkes. *Advances in imaging and electron physics*, volume 116. Academic Press, 2001.
9. Moses Amadasun and Robert King. Textural features corresponding to textural properties. *IEEE transactions on systems, man, and cybernetics*, 19(5):1264–1274, 1989.
10. Menglong Ye, Stamatia Giannarou, Alexander Meining, and Guang-Zhong Yang. Online tracking and retargeting with applications to optical biopsy in gastrointestinal endoscopic examinations. *Medical image analysis*, 30:144–157, 2016.